Author/s:
Hildebrand, MS;Tankard, R;Gazina, EV;Damiano, JA;Lawrence, KM;Dahl, HHM;Regan, BM;Shearer, AE;Smith, RJH;Marini, C;Guerrini, R;Labate, A;Gambardella, A;Tinuper, P;Lichetta, L;Baldassari, S;Bisulli, F;Pippucci, T;Scheffer, IE;Reid, CA;Petrou, S;Bahlo, M;Berkovic, SF

Title:
PRIMA1 mutation: A new cause of nocturnal frontal lobe epilepsy

Date:
2015-08-01

Citation:
Hildebrand, M. S., Tankard, R., Gazina, E. V., Damiano, J. A., Lawrence, K. M., Dahl, H. H. M., Regan, B. M., Shearer, A. E., Smith, R. J. H., Marini, C., Guerrini, R., Labate, A., Gambardella, A., Tinuper, P., Lichetta, L., Baldassari, S., Bisulli, F., Pippucci, T., Scheffer, I. E. ,... Berkovic, S. F. (2015). PRIMA1 mutation: A new cause of nocturnal frontal lobe epilepsy. Annals of Clinical and Translational Neurology, 2 (8), pp.821-830. https://doi.org/10.1002/acn3.224.

Persistent Link:
https://hdl.handle.net/11343/257711

ANNALS of Clinical and Translational Neurology
Open Access
ANA American Neurological Association since 1875

RESEARCH ARTICLE

PRIMA1 mutation: a new cause of nocturnal frontal lobe epilepsy

Michael S. Hildebrand[1], Rick Tankard[2], Elena V. Gazina[3], John A. Damiano[1], Kate M. Lawrence[1], Hans-Henrik M. Dahl[1], Brigid M. Regan[1], Aiden Eliot Shearer[4], Richard J. H. Smith[4], Carla Marini[5], Renzo Guerrini[5], Angelo Labate[6,7], Antonio Gambardella[6,7], Paolo Tinuper[8], Laura Lichetta[8], Sara Baldassari[8], Francesca Bisulli[8], Tommaso Pippucci[8], Ingrid E. Scheffer[1,9], Christopher A. Reid[3], Steven Petrou[3], Melanie Bahlo[2] & Samuel F. Berkovic[1]

[1]Epilepsy Research Centre, Department of Medicine, Austin Health, University of Melbourne, Melbourne, Victoria, Australia
[2]Bioinformatics Division, The Walter and Eliza Hall Institute, Melbourne, Victoria, Australia
[3]The Florey Institute for Neuroscience and Mental Health, The University of Melbourne, Melbourne, Victoria, Australia
[4]Molecular Otolaryngology & Renal Research Laboratories, Department of Otolaryngology-Head and Neck Surgery, University of Iowa Hospitals and Clinics, Iowa City, Iowa
[5]Pediatric Neurology and Neurogenetics Unit and Laboratories, A. Meyer Children's Hospital-University of Florence, Florence, Italy
[6]Institute of Neurology, University Magna Græcia, Catanzaro, Italy
[7]Institute of Molecular Bioimaging and Physiology of the National Research Council (IBFM-CNR), Germaneto, CZ, Italy
[8]Medical Genetics Unit, Polyclinic Sant'Orsola-Malpighi and Department of Medical and Surgical Sciences, University of Bologna, Bologna, Italy
[9]Department of Paediatrics, Royal Children's Hospital, University of Melbourne, Melbourne, Victoria, Australia

Correspondence
Samuel F. Berkovic, Epilepsy Research Centre, Level 2, Melbourne Brain Centre, 245 Burgundy St. Heidelberg, Victoria 3084, Australia. Tel: +61 3 9035 7093; Fax: +61 3 9496 2291; E-mail: s.berkovic@unimelb.edu.au

Funding Information
This study was supported by the National Health and Medical Research Council (NHMRC) Program Grant (628952) to S. F. B., S. P. and I. E. S., an Australia Fellowship (466671) to S. F. B, a Practitioner Fellowship (1006110) to I. E. S and a Career Development Fellowship (1063799) to M. S. H. M. B. was supported by an Australian Research Council (ARC) Future Fellowship (FT100100764) and NHMRC Program Grant (APP1054618), and R. T. by an NHMRC Australian Postgraduate Award. This work was also supported by the Victorian State Government Operational Infrastructure Support and Australian Government NHMRC IRIISS funding to M. B., and a Telethon Foundation Project GGP13200 to P. T. and T. P.

Received: 10 April 2015; Revised: 21 May 2015; Accepted: 29 May 2015.

Annals of Clinical and Translational Neurology **2015; 2(8): 821–830**

doi: 10.1002/acn3.224

Abstract

Objective: Nocturnal frontal lobe epilepsy (NFLE) can be sporadic or autosomal dominant; some families have nicotinic acetylcholine receptor subunit mutations. We report a novel autosomal recessive phenotype in a single family and identify the causative gene. **Methods**: Whole exome sequencing data was used to map the family, thereby narrowing exome search space, and then to identify the mutation. **Results**: Linkage analysis using exome sequence data from two affected and two unaffected subjects showed homozygous linkage peaks on chromosomes 7, 8, 13, and 14 with maximum LOD scores between 1.5 and 1.93. Exome variant filtering under these peaks revealed that the affected siblings were homozygous for a novel splice site mutation (c.93+2T>C) in the *PRIMA1* gene on chromosome 14. No additional *PRIMA1* mutations were found in 300 other NFLE cases. The c.93+2T>C mutation was shown to lead to skipping of the first coding exon of the *PRIMA1* mRNA using a minigene system. **Interpretation**: PRIMA1 is a transmembrane protein that anchors acetylcholinesterase (AChE), an enzyme hydrolyzing acetycholine, to membrane rafts of neurons. PRiMA knockout mice have reduction of AChE and accumulation of acetylcholine at the synapse; our minigene analysis suggests that the c.93+2T>C mutation leads to knockout of *PRIMA1*. Mutations with gain of function effects in acetylcholine receptor subunits cause autosomal dominant NFLE. Thus, enhanced cholinergic responses are the likely cause of the severe NFLE and intellectual disability segregating in this family, representing the first recessive case to be reported and the first *PRIMA1* mutation implicated in disease.

Introduction

Nocturnal frontal lobe epilepsy (NFLE) is characterized by frequent, sometimes violent, and often brief seizures at night, that usually commence during childhood. It can arise sporadically or be inherited in an autosomal dominant fashion (ADNFLE).[1] Clinical features associated with nocturnal seizures include vocalizations, complex and often violent automatisms, and ambulation, making the condition sometimes difficult to distinguish from parasomnias.[2] Electroencephalography (EEG) is often unrevealing, and magnetic resonance imaging (MRI) typically shows no lesions in patients with NFLE. In some cases NFLE is accompanied by intellectual disability and psychiatric disorders, the pathogenic mechanisms of which remain unclear.[2–4]

A minority of ADNFLE cases are due to mutations in three genes (*CHRNA2*, *CHRNA4* and *CHRNB2*) that encode the α2, α4 and β2 subunits of the neuronal nicotinic acetylcholine receptor.[5–7] More recently, mutations in the sodium-activated potassium channel KCNT1[8] were shown to cause a small number of severe familial and sporadic cases. Mutations in the mTOR signaling protein DEPDC5 may also present with NFLE, including in 13% of families in one study.[9–12] The etiology of other familial NFLEs remain to be elucidated, but additional genes are expected to be involved. Gain of function of mutated nicotinic cholinergic receptors appears to be the common mechanism in in vitro studies of human mutations.[5,13] Based on this electrophysiological data, and the genetic data above, other proteins of the cholinergic nervous system may be involved in the pathogenesis of NFLE.

Herein we report a small Australian family of Italian origin segregating autosomal recessive NFLE (ARNFLE) and intellectual disability. Using a methodology we recently reported[14] we performed linkage analysis with whole exome sequencing data to map the disorder to multiple genomic loci, and then, using the same sequence data, we identified the causative gene mutation on chromosome 14. The mutated gene, *PRIMA1*, encodes a proline-rich transmembrane protein that efficiently transforms secreted acetylcholinesterase (AChE) into an enzyme anchored on the outer cell surface.

Materials and Methods

Family and sporadic cases

A two-generation Australian family of Italian origin with NFLE and intellectual disability was studied (Fig. 1). The Human Research Ethics Committee of Austin Health, Melbourne, Australia, approved this study. Informed consent was obtained from living subjects or their relatives.

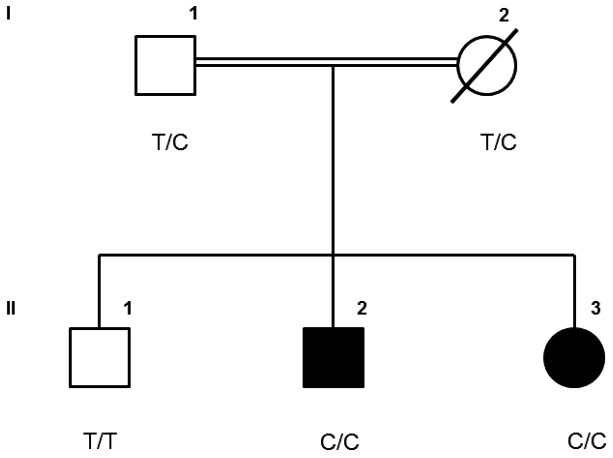

Figure 1. Pedigree of Australian family. Two-generation Australian family of Italian origin segregating ARNFLE (autosomal recessive nocturnal frontal lobe epilepsy) and intellectual disability showing genotypes of the *PRIMA1* c.93+2 nucleotide. Open symbols unaffected; shaded symbols affected; double line consanguineous event; diagonal line deceased. A breast tissue sample was available from individual I:2 for genotyping by Sanger sequencing; blood samples were obtained from the other family members (I:1, II-1, II-2 and II-3), and these samples were exome sequenced.

For re-sequencing experiments, 300 sporadic patients diagnosed with NFLE were collected and phenotyped including 212 cases with Italian ancestry.

Patient samples

Whole blood was obtained and genomic DNA extracted using a Qiagen QIAamp DNA Maxi Kit (Valencia, CA). For individual I:2, who died of breast cancer, paraffin-embedded breast tissue was available for genotyping. The paraffin was removed by treatment with xylene and DNA extracted using phenol chloroform as described previously.[15] Fresh whole blood samples were obtained from affected individual II:3 and her unaffected brother II:1 to generate a lymphoblastoid cell line (LCL) for transcript studies.

Whole exome sequencing

Exome sequencing was performed using 3 μg of venous blood-derived genomic DNA from each of four family members (I:1, II-1, II-2 and II-3; Fig. 1). Genomic DNA was sonicated to approximately 200 base pair (bp) fragments and adaptor-ligated to make a library for paired-end sequencing. Following amplification and barcoding, the libraries were hybridized to biotinylated complementary RNA oligonucleotide baits from the SureSelect Human All Exon 50 Mb Kit (Agilent Technologies, Santa Clara, CA) and purified using streptavidin-bound

magnetic beads as described previously.[16] Amplification was conducted prior to sequencing on the Illumina HiSeq 2000 system (San Diego, CA). The exome design covers 50 megabases of human genome that includes all exons annotated in the GENCODE project (reference annotation for the ENCODE project; Wellcome Trust Sanger Institute) and consensus CDS database (CCDS – March 2009) as well as 10 bp of flanking sequence for each targeted region and small noncoding RNAs from miRBase (http://www.mirbase.org/) (v.13) and Rfam (http://rfam.xfam.org/).

Whole exome analysis and linkage mapping

Exome sequencing reads were aligned with Novoalign version 3.02.00 (http://www.novocraft.com/) to the human genome assembly with ambiguous SNPs (hg19 dbSNP132-masked, UCSC Genome Browser). PCR duplicates were removed using MarkDuplicates from Picard (http://picard.sourceforge.net).

For linkage analysis, a previously described method was used.[14] Briefly, genotypes of SNPs at HapMap Phase II loci[17,18] were inferred using GATK UnifiedGenotyper[19,20] with a required minimum depth of 10 reads per sample, to produce variant call format (VCF) files. LINKDATAGEN[17] produced files for linkage, including removing Mendelian errors. To satisfy linkage equilibrium assumptions markers were chosen so that they were approximately 0.3 cM apart when available. Inbreeding coefficients (F) were estimated using the FEstim[21] algorithm. The estimated inbreeding coefficients were used to generate an appropriate pedigree with an inbreeding loop (Fig. 1) for homozygosity mapping. Multipoint parametric linkage analysis using exome genotypes was performed using MERLIN[22] with a fully penetrant recessive disease model with disease allele frequency 0.00001, with the pedigree described in Figure 1 for homozygosity mapping, and the nuclear family for recessive disease model mapping.

Variant detection was performed with GATK HaplotypeCaller and variant annotation using ANNOVAR.[23] Exome variants were filtered and selected according to the following criteria for the homozygous and compound heterozygous recessive models: location within a linkage region, genotypes fitting the disease model, a minor allele frequency $\leq$0.01 (0.05) in the exome variant server dataset (http://evs.gs.washington.edu/EVS/) and 1000 Genomes,[24] a minor allele frequency of $\leq$0.05 in the Exome Aggregation Consortium database, appearance in <10 alleles of our in-house exome dataset, and mutation type (missense, nonsense, coding indel or splice site variant). Compound heterozygous variants were filtered at the gene level, where candidate genes had to have at least two remaining variants after filtering. Variants in the same gene were assessed pairwise requiring that exactly one variant was heterozygous in the father (I:1), no more than one variant was observed in the unaffected sibling (II:1), and not present in cis-phase as assessed in IGV,[25,26] when possible.

Table 1. Oligonucleotides used in this study.

Target	Oligonucleotide (5′-3′)
PRIMA1 exon 1	CTGACCCTAGCCTTGCTCTC (forward)
	AGGAGGGAAGGGACAGCT (reverse)
PRIMA1 exon 2	CAGCTTCTAGTTGCCTTATGGTC (forward)
	CTCAGTGGATCTTCGTGGG (reverse)
PRIMA1 exon 3	CATGACCAGCTCATCCAGG (forward)
	ATGTGTGTAGGAGCCCCAA (reverse)
PRIMA1 exon 4	ACTAATGGTGTCCCTGCCTC (forward)
	ACCTGCTTTCCCATGTCCAC (reverse)

PCR and sanger sequencing

The *PRIMA1* gene and exome variants were amplified using gene-specific primers (Table 1) designed to the reference human gene transcripts (NCBI Gene; http://www.ncbi.nlm.nih.gov/). Amplification reactions were cycled using a standard protocol on a Veriti Thermal Cycler (Applied Biosystems, Carlsbad, CA) at 60°C annealing temperature for 1 min. Bidirectional sequencing of all exons and flanking regions was completed with a BigDye™ v3.1 Terminator Cycle Sequencing Kit (Applied Biosystems), according to the manufacturer's instructions. Sequencing products were resolved using an 3730× L DNA Analyzer (Applied Biosystems). All sequencing chromatograms were compared to published cDNA sequence; nucleotide changes were detected, using Codon Code Aligner (CodonCode Corporation, Dedham, MA).

Generation and analysis of lymphoblastoid cells

Immortalized lymphoblastoid cell lines were established from venous blood of family members II:1 and II:3 using Epstein–Barr virus and maintained in RPMI-1640 medium supplemented with 20% fetal calf serum. RNA was extracted from the cells using an RNeasy Minikit (Qiagen) and cDNA generated using a SuperScript III First-Strand Synthesis System (LifeTechnologies, Grand Island, NY) according to the manufacturer's instructions. PCR was performed as described above using oligonucleotides designed to *PRIMA1* mRNA and products were resolved on 2% agarose gels.

Minigene assay

Minigenes were generated using Exontrap vector (MoBiTec Molecular Biotechnology, Goettingen, Germany), which includes a 5′ and a 3′ exon separated by a 600 bp

intron containing a polylinker for cloning of DNA of interest. Wild-type and mutant (c.93+2T>C) *PRIMA1* fragments were amplified from genomic DNA of family members II:1 and II:3, respectively, using PCR with the primers 5′-AGGCTTGGTTTACTAGGGTG (forward) and 5′-GAGAACCA**ACTAGT**GGGGTGGCTGCAAGA (reverse, introduced SpeI site is highlighted in bold). The PCR products were digested with XmaI (restriction site is located in intron 1–2) and SpeI, and cloned into XmaI/SpeI-digested polylinker of Exontrap vector. The resulting minigenes contained 307 bp fragment of *PRIMA1*: exon 2 (124 bp) with flanking intronic sequences (83 bp of intron 1–2 and 100 bp of intron 2–3). The minigene sequences were confirmed by Sanger sequencing.

HEK293T cells (a human embryonic kidney cell line stably transfected with the SV40 large T antigen) were maintained in Dulbecco's Modified Eagle's Medium (Invitrogen, Carlsbad, CA) supplemented with 10% (v/v) fetal bovine serum, 100 U/mL penicillin, 100 μg/mL streptomycin, and 2 mmol/L glutamine. The cells were transfected with wild-type or mutant *PRIMA1* minigenes, or empty Exontrap vector, using Lipofectamine-2000™ (Invitrogen). Twenty-four or 48 h post-transfection the cells were harvested and total RNA was extracted using an RNeasy Minikit (Qiagen). cDNA was generated from 1 μg of total RNA using SuperScript III reverse transcriptase and random hexamer primers (Invitrogen). PCR was performed on the cDNA using Platinum High Fidelity Taq (Invitrogen) with the primers binding to the 5′ and 3′ exons of Exontrap vector. The resulting PCR products were analyzed by electrophoresis on a 2% agarose gel.

Results

Clinical details

Two of three siblings with unaffected parents, who were born in the same small Italian village, were diagnosed with NFLE and intellectual disability (Fig. 1). Both required long-term institutional care. The 53 year-old female proband (II:3) had a history of motor and speech delay, short stature, ataxic gait, congenital nystagmus, and a squint. Chromosome analysis, metabolic screening and computed tomography (CT) were normal in childhood. During early childhood she developed seizures that persisted throughout adult life. The predominant attacks were nocturnal hyperkinetic seizures with duration ~1–2 min and a frequency of 1–2 per week characterized by loud vocalizations, bilateral asymmetrical limb movements, often with incontinence and postictal confusion. Occasional generalized convulsions also occurred. Examination revealed nystagmus, moderate intellectual disability, and a broad-based gait without other specific cerebellar signs. Video electrocephalogram (EEG) confirmed frontal lobe nocturnal hyperkinetic attacks, and diurnal staring attacks thought to be behavioral. CT scans and MRI brain showed no specific lesions; there was a suggestion of mild cerebellar atrophy. Her clinical course was relatively stable over the last two decades.

Her 61-year-old affected brother (II:2) shares many clinical features with his sister. He had congenital nystagmus and developed epilepsy in early childhood characterized by monthly ~1–2-min nocturnal seizures with vocalization, asymmetrical limb movements and postictal drowsiness as well as brief generalized tonic-clonic seizures in the early morning or late evening. Clinical evaluation revealed moderate intellectual disability, nystagmus, and a mild-ataxic gait. EEG showed slow, poorly sustained posterior dominant rhythm, delta slowing, with bifrontal epileptiform discharges. Brain CT revealed mild cerebral and cerebellar atrophy. He required a number of hospitalizations for poor seizure control.

Candidate gene screening

The coding regions and splice sites of three known ADNFLE genes – *CHRNA2*, *CHRNA4*, and *CHRNB2* – were Sanger sequenced without identification of a causal mutation. The *KCNT1* and *DEPDC5* genes were discovered to be causal NFLE genes only after this study commenced and no mutation of these genes was found in the subsequent exome sequencing analysis.

Linkage mapping using exome data detects multiple genomic loci

The inheritance pattern in the family was unclear although a recessive mode appeared most likely. We performed linkage analysis with a fully penetrant recessive model using 7102 SNP markers generated from the exomes of four family members (I:1, II:1, II:2 and II:3; Fig. 1). We tested the hypothesis that the family was consanguineous and FEstim analysis indicated that the parents were related (F estimates 0.034, 0.021, 0.036 (SE 0.010, 0.009, 0.014) for II:1, II:2, and II:3, respectively), with an inferred relationship of second-cousins. The father (I:1) also showed evidence of consanguinity (F = 0.022 [SE 0.009]), but his inbreeding loop is not relevant to the detection of autozygosity for this phenotype. Multipoint parametric linkage analysis using a pedigree with an inferred inbreeding loop revealed multiple linkage peaks including four with a parametric LOD score >1.5 (Fig. 2A; Table 2), and using the nuclear pedigree produced 36 regions with LOD score >0.5 (Fig. 2B; Table 3), allowing us to exclude 98 and 74% of the autosome, respectively.

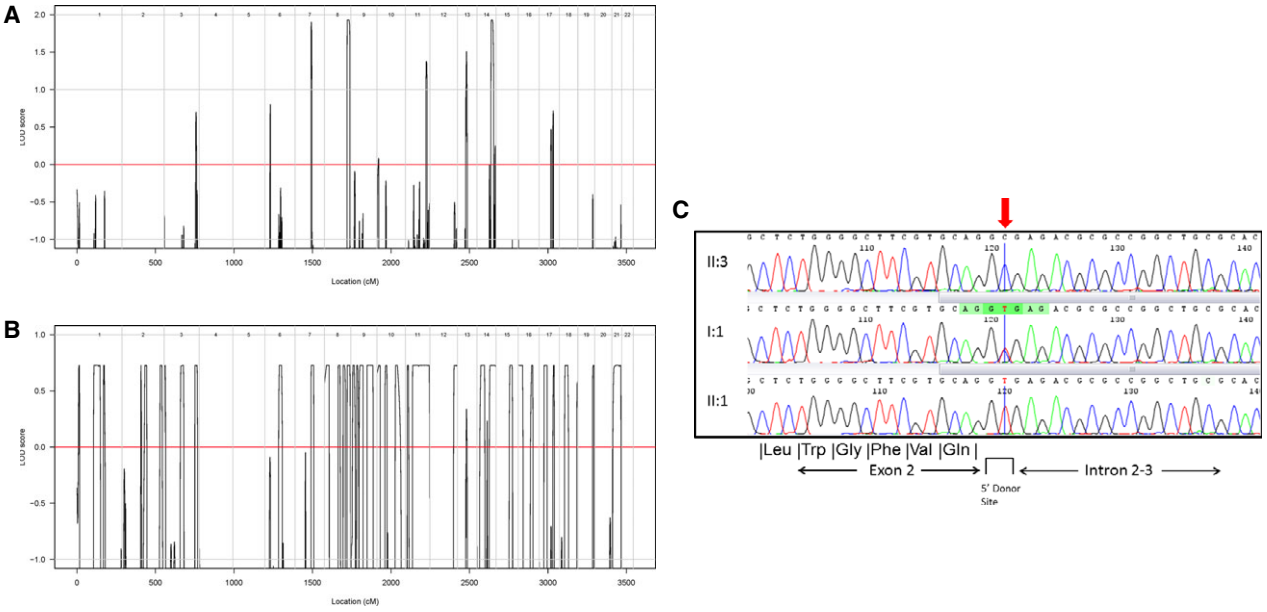

Figure 2. Whole exome sequencing and linkage mapping. (A) Genome-wide parametric LOD scores generated using exome data assuming an autosomal recessive inheritance model with consanguinity. Multiple linkage peaks were detected with the highest LOD score of ~1.93 detected for regions on chromosomes 8 and 14. (B) Genome-wide parametric LOD scores generated using exome data assuming an autosomal recessive inheritance model with the nuclear pedigree. Multiple linkage peaks were detected with the highest LOD score of ~0.71. (C) Representative sequence chromatograms of c.93+2 genotypes in the family – the results for three individuals are shown.

Exome variant analysis reveals a mutation in the *PRIMA1* gene

We generated high coverage exomes for all four family members (Table 4). Exome variants under the linkage peaks were filtered as described in the Methods section where one homozygous recessive and twelve compound heterozygous variants in one and six genes, respectively, were identified that passed filtering (Tables 5, 6). The homozygous variant on chromosome 14 in the *PRIMA1* gene is a novel splice site mutation (c.93+2T>C) that substitutes the invariant 'T' allele[27] of the 5′ splice site of the intron following exon 2 (the first coding exon) for a 'C' (Fig. 2C). This mutation is predicted to cause skipping of exon 2 during *PRIMA1* pre-mRNA splicing as supported by splice prediction software (Analzyer Splice Site Tool, Tel Aviv University, Israel) indicating the splicing machinery will fail to recognize the mutant splice site. Since individual I:2 was not exome sequenced, her c.93+2 genotype was determined by Sanger sequencing of genomic DNA derived from her breast tissue (Fig. 1). Although *PRIMA1* lymphocyte expression was not reported in publicly available expression databases, we obtained a fresh blood sample from affected (II:3) and unaffected (II:1) sibs and generated lymphoblastoid cell lines (LCLs) to check for mRNA expression. However, *PRIMA1* expression was not detected in cell lines from either family member (data not shown).

Table 2. Chromosomal regions with LOD > 1.5 identified by homozygosity mapping.

	Flanking genetic markers						
	Beginning of region			End of region			Peak LOD
Chr	Marker	Base pairs	cM	Marker	Base pairs	cM	Parametric
7	rs17241389	83,764,309	101.32	rs2106432	92,970,847	107.25	1.8970
8	rs3935174	131,165,086	144.37	rs2292781	141,559,358	161.5	1.9264
13	rs7997193	56,574,363	55.7	rs9541675	69,559,370	63.66	1.5088
14	rs3818263	92,588,002	90.12	rs1047351	99,876,505	106.71	1.9263

chr, chromosome; cM, centimorgan.

Table 3. Chromosomal regions with LOD > 0.5 identified by recessive disease model mapping.

	Flanking genetic markers						
	Beginning of region			End of region			Peak LOD
Chr	Marker	Base pairs	cM	Marker	Base pairs	cM	Parametric
1	rs12127966	4,234,940	9.937	rs6689940	6,281,090	15.914	0.7084
1	rs2803155	77,958,837	106.42	rs541628	117,256,763	147.404	0.7085
1	rs11264818	157,742,017	168.503	rs10800465	162,310,313	175.048	0.7085
2	rs6716306	102,014,754	120.716	rs13427053	105,186,053	123.054	0.7083
2	rs13020764	125,664,440	144.186	rs4525749	139,069,573	157.912	0.7085
2	rs6436746	228,893,467	242.144	rs10169296	236,766,825	256.37	0.7085
3	rs2674533	651,876	0.799	rs1562080	4,025,703	10.174	0.7083
3	rs9873219	77,354,463	104.709	rs9873303	115,396,528	125.341	0.7085
3	rs7633364	185,218,549	196.279	rs2280268	193,031,926	213.549	0.7085
6	rs9448707	80,139,318	88.977	rs9391249	105,343,433	108.871	0.7085
7	rs1429745	85,005,512	101.86	rs4727629	105,467,529	118.864	0.7085
8	rs17745485	417,836	0.383	rs5020778	13,596,612	30.377	0.7084
8	rs7836437	70,840,655	87.368	rs10098671	87,243,097	100.132	0.7085
8	rs7830253	108,185,786	119.456	rs16899173	124,995,902	133.622	0.7084
8	rs13278110	131,097,405	144.368	rs11167136	143,310,815	164.929	0.7085
9	rs4237150	4,290,085	11.461	rs4741080	11,009,202	25.175	0.7085
9	rs3824372	17,752,252	36.778	rs17781724	24,538,114	46.728	0.7085
9	rs7850371	28,164,681	53.241	rs12238895	80,827,249	78.289	0.7085
9	rs10988451	101,741,666	103.679	rs4240435	132,385,003	142.573	0.7085
10	rs1769236	734,229	0.192	rs4749890	9,739,317	21.719	0.7085
10	rs17685697	28,620,873	51.218	rs1961333	45,612,064	64.193	0.7079
10	rs1547843	91,738,263	117.5	rs4463806	115,597,993	140.176	0.7085
11	rs325606	6,243,982	12.483	rs9787738	11,161,897	20.532	0.7085
11	rs17609863	29,293,934	46.016	rs11601550	133,707,109	155.667	0.7085
12	rs4765268	126,133,693	151.605	rs12300232	133,648,090	174.669	0.7085
14	rs1984536	26,637,188	18.918	rs11623717	54,414,132	48.798	0.7085
14	rs7150314	82,384,079	77.741	rs4448834	107,170,398	120.134	0.7085
15	rs453151	70,097,675	86.294	rs3743475	89,172,558	105.572	0.7085
16	rs7359494	310,574	0.172	rs3748980	12,875,075	29.646	0.7085
16	rs11643526	61,668,000	80.826	rs8044379	76,274,993	94.041	0.7085
17	rs11651333	11,858,949	30.461	rs11656692	31,327,572	50.541	0.7085
17	rs4128941	63,531,331	89.185	rs7211813	68,144,014	96.289	0.7085
18	rs2293517	10,784,331	32.578	rs11662426	36,920,736	56.684	0.7085
18	rs5375	74,962,810	111.193	rs9950415	77,643,034	117.589	0.5693
19	rs11881257	54,196,217	93.877	rs12691095	56,718,895	103.318	0.7085
21	rs9981410	17,450,982	5.82	rs1005164	45,680,103	58.637	0.7085

chr, chromosome; cM, centimorgan.

None of the six genes containing compound heterozygous variants (Table 6) are convincing candidates. For *LOC120824*, nothing is known while little functional information is available for *DNHD1*, other than it encodes the dynein heavy chain domain 1 that is predicted to be a chaperone or mitotic protein,[28] and *CLEC16A*, other than it is a susceptibility gene for diabetes, multiple sclerosis, and immunoglobulin A deficiency.[29] *ABCA8* is a xenobiotic transporter gene of the ABC subfamily that transport foreign chemicals, such as antibiotics, across cellular membranes by ATP hydrolysis.[30] *PPL* encodes periplakin that is expressed in brain but its known function is to associate with desmosomal plaques and keratin filaments in the epidermis, and mice null for the gene are phenotypically normal.[31] A tumor suppressor gene, *LLGL1* regulates basal protein targeting in both embryonic and larval Drosophila neuroblasts,[32] and newborn homozyous knockout Lgl1 pups develop severe hydrocephalus and die neonatally.[33]

Confirmation of *PRIMA1* exon skipping in vitro

Since *PRIMA1* was not expressed in lymphocytes and we did not have access to other tissues from family members, we examined the effect of the mutation using a minigene

Table 4. Exome coverage statistics.

Patient	Total reads	Mean read depth	% bases covered by 2 reads	% bases covered by 5 reads	% bases covered by 10 reads
I:1	2278520917	44	94	91	85
II:1	3801912357	73	96	94	91
II:2	1802808122	35	94	89	81
II:3	5292190911	102	96	94	92

Table 5. Filtered homozygous recessive exome variants under linkage peaks.

Chr	Genomic site	Variant	Gene	Amino acid	Effect
14	94,253,970	T>C	*PRIMA1*	–	Splice site

assay. *PRIMA1* DNA fragments containing exon 2 (124 bp) with flanking intronic sequences (wild-type and c.93+2T>C) were amplified from the genomic DNA of unaffected and affected family members, respectively, and cloned into a splicing-competent minigene vector. HEK293T cells were transfected with the minigenes and the vector, and incubated for 24 or 48 h. Cellular RNA was then extracted and the splicing of minigene-derived RNA was analyzed by RT-PCR using PCR primers binding to the 5′ and 3′ exons of the vector. The results revealed incorporation of exon 2 in RNA produced by the wild-type minigene and skipping of exon 2 in RNA produced by the mutant minigene (Fig. 3).

Re-sequencing of *PRIMA1* in additional cases

We designed oligonucleotides (Table 1) to screen the entire coding region and splice sites of the *PRIMA1* gene. Three hundred unrelated patients diagnosed with NFLE, including 212 with Italian ancestry, were screened using these oligonucleotides by Sanger sequencing or as part of the exome sequencing studies. No potential recessive or compound heterozygous mutations were detected.

Discussion

Nocturnal frontal lobe epilepsy is an important epilepsy syndrome known to be inherited in an autosomal dominant manner or to occur sporadically. Recessive inheritance has not been previously recognized. Using a whole exome and linkage analysis strategy, we discovered the cause for ARNFLE and intellectual disability in this family, being a mutation in the *PRIMA1* gene.

Acetylcholinesterase (AChE) plays a pivotal role as a hydrolase in the central and peripheral nervous systems catalyzing the hydrolysis of acetylcholine (ACh) to maintain neurotransmitter homeostasis. Inhibition of AChE leads to enhanced cholinergic responses due to excess ACh over-stimulating nicotinic and muscarinic receptors.[34] This can alter both central and peripheral processes, including control of respiration and seizure activity, autonomic, and somatic motor functions. In brain, AChE is found in its functional form as a tetramer associated with PRIMA1 at neuronal synapses. This association is facilitated by interaction between the tryptophan amphiphilic tetramerization domains on the catalytic subunits of AChE and the proline-rich attachment domain (PRAD) on the extracellular domain of PRIMA1.[35]

Perturbation of the cholinergic system has been linked to the pathogenesis of ADNFLE, specifically the increased sensitivity of nicotinic acetylcholine receptor (nAChR) subunits to ACh. Dominant mutations in three receptor subunits have been found in families segregating NFLE.[5–7] This hypersensitivity was demonstrated for the α2 subunit mutation in vitro by whole-cell recordings of HEK293 cells transfected with wild-type or mutant receptor.[5] Loss

Table 6. Filtered compound heterozygous exome variants under linkage peaks.

Chr	Genomic site	Variant	Gene	Amino acid	Effect
11	6,519,561	A>G	DNHD1	Q>R	Nonsynonymous SNV
11	6,568,866	C>T	DNHD1	R>C	Nonsynonymous SNV
11	48,997,336	C>T	LOC120824	C>Y	Nonsynonymous SNV
11	49,003,195	C>A	LOC120824	C>F	Nonsynonymous SNV
16	4,934,157	->CCACCTTCTCCTTGACCT	PPL	V>EVKEKVV	Nonframeshift insertion
16	4,945,400	CTC>-	PPL	E>-	Nonframeshift deletion
16	11,097,073	G>C	CLEC16A	G>A	Nonsynonymous SNV
16	11,272,419	C>A	CLEC16A	P>T	Nonsynonymous SNV
17	18,129,027	G>A	LLGL1	A>T	Nonsynonymous SNV
17	18,133,277	A>C	LLGL1	N>T	Nonsynonymous SNV
17	66,879,927	C>T	ABCA8	–	Splice site
17	66,914,289	G>C	ABCA8	P>R	Nonsynonymous SNV

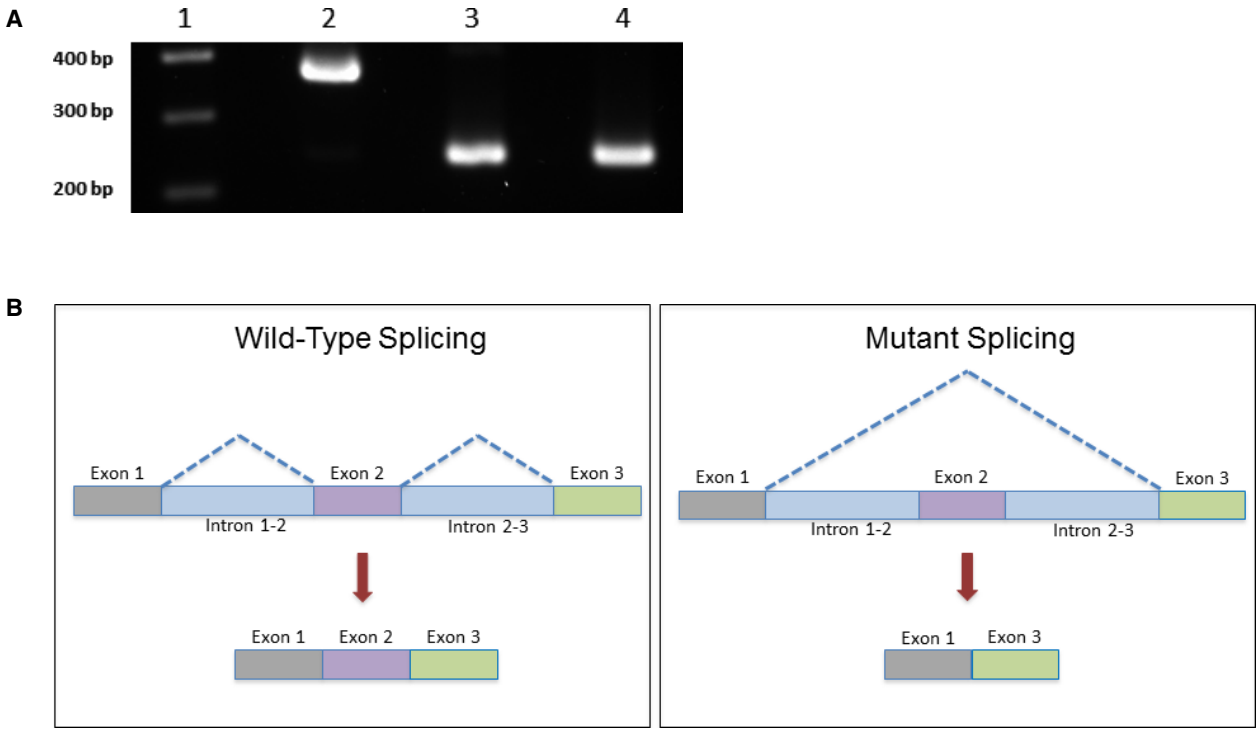

Figure 3. Minigene analysis reveals exon skipping. (A) RT-PCR results showing skipping of the first coding exon of *PRIMA1* due to the c.93+2T>C mutation 48 h following transfection into HEK293T cells. A 100 base pair marker (lane 1) was run. The 124 base pair first exon of *PRIMA1* is only expressed from the wild-type minigene construct (lane 2), resulting in a 369 base pair product. Whereas the mutant (lane 3) and empty vector control (lane 4) both lack the first exon producing 245 base pair products. The same result was observed in cells harvested 24 h posttransfection (data not shown). (B) Schematic illustration of exon skipping caused by the c.93+2T>C mutation compared to the wild-type splicing.

of PRIMA1 represents a new mechanism for overstimulation of nAChRs via reduction in AChE activity leading to accumulation of ACh. A severe reduction in AChE has already been demonstrated in PRiMA knockout mice that lack the critical PRAD domain.[34] In the striatum, chosen because it contains the highest level of AChE in the brain, PRiMA knockout mice only exhibit 2–3% of wild-type AChE activity despite having normal *AChE* mRNA levels. The residual AChE is localized to the endoplasmic reticulum. These data indicate that PRiMA is critical to intracellular processing of AChE, and targeting it to and stabilizing it at the axon. It is noteworthy that PRiMA is only required to anchor AChE at synaptic junctions in the brain, and not in the muscle, consistent with the phenotype observed in the family studied here.

The splice site mutation we found in *PRIMA1* results in skipping of the first coding exon that contains the first 93 base pairs of coding sequence. While in-frame, this would result in loss of the first 31 amino acids of the PRIMA1 protein, including the methionine start site and most of the signal peptide. An alternative methionine start site is not present until position 137, close to the C-terminus of the 153 amino acid PRIMA1 protein. Since the affected siblings are homozygous for the mutation, the effect is predicted to be a complete knockout of PRIMA1 in their cells.

We describe ARNFLE, and document a more severe phenotype than usually observed in dominant cases that includes intellectual disability. Our genetic analysis reveals the first cause for this disease being mutation of *PRIMA1*. Whilst it would have been ideal to identify further independent subjects with mutated *PRIMA1*, analysis of 300 other unrelated cases was negative. However, the likely loss of function of PRIMA1 caused by this mutation and its biological plausibility because of its effect on the cholinergic system strongly suggest it is a novel, albeit rare, cause of NFLE. This further highlights the role of the cholinergic system in this characteristic nocturnal epilepsy syndrome.

Acknowledgments

We thank the family for their participation in this study. Elena Aleksoska (Epilepsy Research Centre) is acknowledged for performing genomic DNA extractions. This study was supported by the National Health and Medical Research Council (NHMRC) Program Grant (628952) to S. F. B., S. P. and I. E. S., an Australia Fellowship (466671) to S. F. B, a Practitioner Fellowship (1006110)

to I. E. S and a Career Development Fellowship (1063799) to M. S. H. M. B. was supported by an Australian Research Council (ARC) Future Fellowship (FT100100764) and NHMRC Program Grant (APP1054618), and R. T. by an NHMRC Australian Postgraduate Award. This work was also supported by the Victorian State Government Operational Infrastructure Support and Australian Government NHMRC IRIISS funding to M. B., and a Telethon Foundation Project GGP13200 to P. T. and T. P.

Author Contributions

S. F. B. initiated the project. M. S. H. and S. F. B. directed the project. M. S. H., A. E. S., R. J. H. S., P. T., L. L. and T. P. performed exome sequencing, and R. T. and M. B. performed exome data analysis. J. A. D., H. H. M. D., R. G., A. L., A. G., T. P., P. T., L. L., F. B., and T. P. performed variant validation by Sanger sequencing. K. M. L., B. M. R., C. M., R. G., A. L., A. G., T. P., P. T., L. L., F. B., T. P., I. E. S., and S. F. B. conducted clinical phenotyping. E. V. G., M. S. H., J. A. D., C. A. R., and S. P. constructed minigenes and completed splicing assays. M. S. H. and S. F. B. wrote the paper. All authors discussed the results and commented on the manuscript.

Conflict of Interest

Authors report grant funds that contributed to this project as outlined in the Acknowledgements section. I. E. S. discloses payments from UCB Pharma, Athena Diagnostics and Transgenomics for lectures and educational presentations. S. F. B. discloses payments from UCB Pharma, Novartis Pharmaceuticals, Sanofi-Aventis, and Jansen Cilag for lectures and educational presentations, and a patent for SCN1A testing held by Bionomics Inc and licensed to various diagnostic companies.

References

1. Scheffer IE, Bhatia KP, Lopes-Cendes I, et al. Autosomal dominant nocturnal frontal lobe epilepsy. A distinctive clinical disorder. Brain 1995;118(Pt 1):61–73.
2. Derry CP, Davey M, Johns M, et al. Distinguishing sleep disorders from seizures: diagnosing bumps in the night. Arch Neurol 2006;63:705–709.
3. Cho YW, Motamedi GK, Laufenberg I, et al. A Korean kindred with autosomal dominant nocturnal frontal lobe epilepsy and mental retardation. Arch Neurol 2003;60:1625–1632.
4. Khatami R, Neumann M, Schulz H, Kolmel HW. A family with autosomal dominant nocturnal frontal lobe epilepsy and mental retardation. J Neurol 1998;245:809–810.
5. Aridon P, Marini C, Di Resta C, et al. Increased sensitivity of the neuronal nicotinic receptor alpha 2 subunit causes familial epilepsy with nocturnal wandering and ictal fear. Am J Hum Genet 2006;79:342–350.
6. De Fusco M, Becchetti A, Patrignani A, et al. The nicotinic receptor beta 2 subunit is mutant in nocturnal frontal lobe epilepsy. Nat Genet 2000;26:275–276.
7. Steinlein OK, Mulley JC, Propping P, et al. A missense mutation in the neuronal nicotinic acetylcholine receptor alpha 4 subunit is associated with autosomal dominant nocturnal frontal lobe epilepsy. Nat Genet 1995;11:201–203.
8. Heron SE, Smith KR, Bahlo M, et al. Missense mutations in the sodium-gated potassium channel gene KCNT1 cause severe autosomal dominant nocturnal frontal lobe epilepsy. Nat Genet 2012;44:1188–1190.
9. Dibbens LM, de Vries B, Donatello S, et al. Mutations in DEPDC5 cause familial focal epilepsy with variable foci. Nat Genet 2013;45:546–551.
10. Ishida S, Picard F, Rudolf G, et al. Mutations of DEPDC5 cause autosomal dominant focal epilepsies. Nat Genet 2013;45:552–555. DOI:10.1038/ng.2601
11. Picard F, Makrythanasis P, Navarro V, et al. DEPDC5 mutations in families presenting as autosomal dominant nocturnal frontal lobe epilepsy. Neurology 2014;82:2101–2106. DOI:10.1212/WNL.0000000000000488
12. Scheffer IE, Heron SE, Regan BM, et al. Mutations in mTOR regulator DEPDC5 cause focal epilepsy with brain malformations. Ann Neurol 2014;75:782–787.
13. Bertrand D, Picard F, Le Hellard S, et al. How mutations in the nAChRs can cause ADNFLE epilepsy. Epilepsia 2002;43(suppl 5):112–122.
14. Smith KR, Bromhead CJ, Hildebrand MS, et al. Reducing the exome search space for Mendelian diseases using genetic linkage analysis of exome genotypes. Genome Biol 2011;12:R85.
15. Grimberg J, Nawoschik S, Belluscio L, et al. A simple and efficient non-organic procedure for the isolation of genomic DNA from blood. Nucleic Acids Res 1989;17:8390.
16. Zheng J, Miller KK, Yang T, et al. Carcinoembryonic antigen-related cell adhesion molecule 16 interacts with alpha-tectorin and is mutated in autosomal dominant hearing loss (DFNA4). Proc Natl Acad Sci USA 2011;108:4218–4223.
17. Bahlo M, Bromhead CJ. Generating linkage mapping files from Affymetrix SNP chip data. Bioinformatics 2009;25:1961–1962.
18. Frazer KA, Ballinger DG, Cox DR, et al. A second generation human haplotype map of over 3.1 million SNPs. Nature 2007;449:851–861.
19. DePristo MA, Banks E, Poplin R, et al. A framework for variation discovery and genotyping using next-generation DNA sequencing data. Nat Genet 2011;43:491–498. DOI:10.1038/ng.806
20. McKenna A, Hanna M, Banks E, et al. The Genome Analysis Toolkit: a MapReduce framework for analyzing

next-generation DNA sequencing data. Genome Res 2010;20:1297–1303. DOI:10.1101/gr.107524.110.
21. Leutenegger AL, Prum B, Genin E, et al. Estimation of the inbreeding coefficient through use of genomic data. Am J Hum Genet 2003;73:516–523.
22. Abecasis GR, Cherny SS, Cookson WO, Cardon LR. Merlin–rapid analysis of dense genetic maps using sparse gene flow trees. Nat Genet 2002;30:97–101.
23. Wang K, Li M, Hakonarson H. ANNOVAR: functional annotation of genetic variants from high-throughput sequencing data. Nucleic Acids Res 2010;38:e164.
24. Abecasis GR, Altshuler D, Auton A, et al. A map of human genome variation from population-scale sequencing. Nature 2010;467:1061–1073.
25. Robinson JT, Thorvaldsdottir H, Winckler W, et al. Integrative genomics viewer. Nat Biotechnol 2011;29: 24–26.
26. Thorvaldsdottir H, Robinson JT, Mesirov JP. Integrative Genomics Viewer (IGV): high-performance genomics data visualization and exploration. Brief Bioinform 2013;14:178–192. DOI:10.1093/bib/bbs017
27. Shapiro MB, Senapathy P. RNA splice junctions of different classes of eukaryotes: sequence statistics and functional implications in gene expression. Nucleic Acids Res 1987;15:7155–7174.
28. Taipale M, Tucker G, Peng J, et al. A quantitative chaperone interaction network reveals the architecture of cellular protein homeostasis pathways. Cell 2014;158:434–448. DOI:10.1016/j.cell.2014.05.039
29. Hakonarson H, Grant SF, Bradfield JP, et al. A genome-wide association study identifies KIAA0350 as a type 1 diabetes gene. Nature 2007;448:591–594.
30. Tsuruoka S, Ishibashi K, Yamamoto H, et al. Functional analysis of ABCA8, a new drug transporter. Biochem Biophys Res Commun 2002;298:41–45.
31. Aho S, Li K, Ryoo Y, et al. Periplakin gene targeting reveals a constituent of the cornified cell envelope dispensable for normal mouse development. Mol Cell Biol 2004;24:6410–6418.
32. Peng CY, Manning L, Albertson R, Doe CQ. The tumour-suppressor genes lgl and dlg regulate basal protein targeting in Drosophila neuroblasts. Nature 2000;408:596–600.
33. Klezovitch O, Fernandez TE, Tapscott SJ, Vasioukhin V. Loss of cell polarity causes severe brain dysplasia in Lgl1 knockout mice. Genes Dev 2004;18:559–571.
34. Dobbertin A, Hrabovska A, Dembele K, et al. Targeting of acetylcholinesterase in neurons in vivo: a dual processing function for the proline-rich membrane anchor subunit and the attachment domain on the catalytic subunit. J Neurosci 2009;29:4519–4530. DOI:10.1523/JNEUROSCI. 3863-08.2009
35. Perrier AL, Massoulie J, Krejci E. PRiMA: the membrane anchor of acetylcholinesterase in the brain. Neuron 2002;33:275–285.

